

A Particular Problem of Fin Flutter

Chapter 9

Introduction –

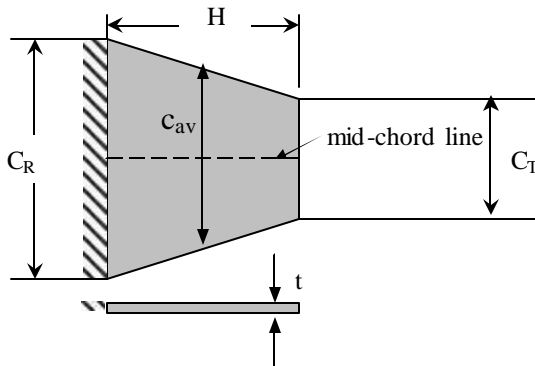
Flutter of an elastic body is a self-excited vibration of that body while immersed in fluid flow. In the case of a rocket, flutter is associated with the aero-elastic characteristics of the fin/body combination while flying through the atmosphere. Flutter is typically the coupled motion of fin twist (torsion), fin plunge (bending) and possibly the rigid and/or flexible motions of the rocket body. Each component of the coupled motion is referred to as a degree-of-freedom. The discussion here will be limited to the motions of the fin itself and any body contribution will be ignored. In essence, it is assumed that the fin is rigidly fixed and cantilevered to an infinitely stiff body structure. Hence, the degrees-of-freedom will be limited to fin torsion and fin bending.

The lowest speed attained when the fin sustains a neutrally stable oscillation is known as the flutter speed. Aero-elastic motions will be damped below flutter speed. At speeds just above the flutter speed, the motion will be divergent in one or both of the degrees-of-freedom. The divergence speed is associated with the minimum speed when both torsion and bending are no longer damped, where one degree-of-freedom is typically divergent and the other is neutrally stable. Structural failure usually occurs at divergence speed. Typically the divergence speed is only slightly greater than the flutter speed. Thus it is important that the prediction of flutter speed be used as a “never-to-exceed” design criterion.

Fin flutter is a complex physical problem to characterize mathematically. Sophisticated structural and aerodynamic tools are typically used to perform flutter analysis. Finite Element Methods (FEM) may be used to characterize both the structure and aerodynamics. Other computational fluid analyses such as Finite Difference or Doublet Lattice Methods (DLM) may be used to characterize the aerodynamics. DLM is commonly used for subsonic flutter analysis. These tools are beyond the scope of this discussion. The discussion here is limited to classical structural and aerodynamic methods. Although the accuracy of the predicted flutter speed may be questionable, the physical trends can be studied.

This study is limited to fins of simple geometry and construction, per the following description:

1. Thin plate of trapezoidal plan form shape
2. Plate thickness to average chord ratio between 0.04 and 0.09 ($0.04 \leq t/c_{av} \leq 0.09$)
3. Homogeneous construction
4. Zero sweep of mid-chord line
5. Fin is rigidly cantilevered at the root chord to rocket body junction
6. The effect of rocket body flexibilities are ignored
7. The effect of rigid body motions are ignored



Where,

H = exposed fin half span
 C_R = exposed fin root chord
 C_T = exposed fin tip chord

Then:

$$I = C_T / C_R = \text{Taper Ratio}$$

$$A = \frac{4H}{(1+I)C_R} = \text{Aspect Ratio}$$

This chapter presents a sequence of discussions that build upon each other to form a flutter analysis method. These discussions are:

1. Fin materials and their properties
2. Natural structural frequency prediction
3. The definition of reduced frequency k
4. Quasi-steady flutter analysis
5. Unsteady flutter analysis
6. Final assessment of example problem

Fin Materials and Their Properties –

Rocket fins in the hobby of rocketry have been built from a variety of materials. Some of the most common materials are polystyrene, balsa, and basswood. These materials will be discussed in this section.

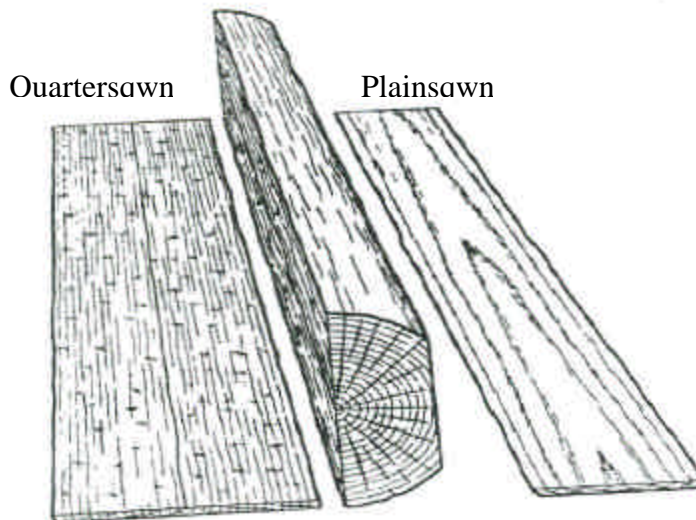
Polystyrene -

Polystyrene is a material that is commonly used in plastic models. It is a homogeneous isotropic material, and thus its mechanical properties are directionally independent. These properties are defined by one value of Young's Modulus (E), one value of shear modulus (G), one value of Poisson's Ratio (ν). Like all materials of this section, its mass is defined by one value of density (ρ_m).

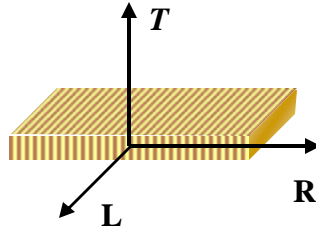
Balsa and Basswood -

Balsa and basswood are examples of natural composite materials having 3D orthotropic characteristics. A material is 3D orthotropic if its mechanical properties can be described in 3 principle orthogonal directions. Because trees grow in concentric annual rings, the 3 principle orthogonal directions are easily defined. One principle direction is along the axis of the trunk. A second principle direction is normal to the concentric annual rings, and the third principle direction is tangent to these rings.

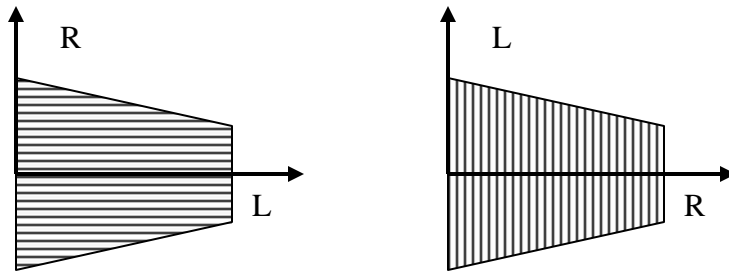
Lumber is typically cut into two distinct configurations: (1) nearly tangent to the annual rings, and (2) nearly parallel to the rays projecting from the trunk center and normal to the annual rings. The first configuration is known as plainsawn and the second as quartersawn. These two configurations are depicted below:



Most balsa and basswood sheet stock cut for use by hobbyists is quartersawn. This discussion will be limited to quartersawn sheet stock. Fiber orientation is a very important consideration for providing the needed stiffness and strength characteristics of rocket fins. The dominant fiber direction is along the axis of the trunk, and is designated as ‘L’ for longitudinal. The least dominant of the directions is tangent to the annual rings and is designated as ‘T’. The remaining direction is radial to the annual rings and is designated as ‘R’. For the quartersawn configuration, these orientations are depicted as follows:



Given a quartersawn sheet stock, one could orient the fiber of a fin layout in any direction within the L-R plane. However, it would be wise to orient the fiber (L-direction) spanwise in order to provide maximum stiffness and strength. The weakest orientation of the fiber would be in the chordwise direction. These two extreme conditions are shown below.



Further discussions will be limited to the situation where the fiber is oriented spanwise.

The fin response in vibration is a result of the complicated interaction between the 3D orthotropic mechanical characteristics. An approach to characterize this vibration is to use Finite Element Analysis (FEA) to account for this interaction, and correlate the results to a semi-empirical approach using a function described by a frequency parameter. The properties used in the semi-empirical approach are as follows:

$E \approx E_L$ = Longitudinal Modulus of Elasticity

$G = \sqrt{G_{LR} G_{LT}}$ = Effective Shear Modulus

G_{LR} = Shear Modulus in the L-R Plane

G_{LT} = Shear Modulus in the L-T Plane

$\nu = \nu_{LR}$ = Poisson's Ratio in the L-R Plane

Material Properties –

The properties to be used in the semi-empirical approach, for the materials just described, are tabulated below. They represent nominal properties. The properties specific to balsa and basswood are from Reference 1, “Wood Handbook – Wood as an Engineering Material”.

Table 1 - Material Properties for Various Fin Materials			
Property	Polystyrene	Balsa	Basswood
Density ρ_m , lbs/in ³	0.038	0.005926	0.013704
Poisson's Ratio ν	0.33	0.229	0.364
Modulus of Elasticity E , lbs/in ²	0.365×10^6	0.539×10^6	1.606×10^6
Shear Modulus G , lbs/in ²	13.722×10^4	2.409×10^4	8.151×10^4

Estimation of the Natural Frequencies –

Required input for the flutter equations include the fin's natural frequencies of vibration in bending and torsion. The oscillatory motion about a state of equilibrium resulting from a disturbing force that is applied once and removed is known as a natural or free vibration. The zero damped frequency associated with free vibration is known as the natural or fundamental frequency, and related to the system stiffness and mass as follows:

$$\omega = \sqrt{\frac{k}{m}}, \text{ Radians per Second}$$

Where,

$$\begin{aligned} k &= \text{System stiffness} \\ m &= \text{System mass} \end{aligned}$$

The natural frequency can be converted to a linear frequency of vibration as follows:

$$f = \frac{\omega}{2\pi}, \text{ Hz or Cycles per Second}$$

The equations for the prediction of these frequencies will be stated, but not derived in this section.

The equations for estimation of the natural frequencies are classified as semi-empirical. Although the basic formulation of the frequency equations is mechanistic (physically based), it also includes an empirical correlation component known as the frequency parameter. The frequency parameter relates (correlates) the basic mechanistic component to either test data and/or a more sophisticated and validated analysis method. It can be stated that the frequency equation consists of an empirical component and a mechanistic component, leading to the classification of semi-empirical.

The frequency parameters presented in this section are derived from correlation of the mechanistic component to results of Finite Element Analyses (FEA). The frequency parameters are found to be a function of fin material and geometry. The fin geometric parameters are aspect ratio (A), taper ratio (I), and thickness-to-chord ratio (t/c). FEA results suggested that the frequency parameters are insensitive to variation in thickness-to-chord ratio, as long as t/c falls into the category of a thin plate ($0.04 \leq t/c \leq 0.09$). For purposes of this study, the effect of t/c on the frequency parameter is ignored.

Natural Frequency in Bending –

The natural frequency in bending can be estimated using the following equation.

$$w_h = K_B \left[\frac{Et^2 g}{12r_m(1-n^2)(1+M_B)} \right]^{1/2} \left[\frac{1}{H^2} \right], \text{ Radians per Second}$$

Where,

E = Young's Modulus, psi

t = Fin thickness, inches

g = Gravity constant, typically 386.088 in/sec²

r_m = Material density, lbs./in³

n = Poisson's ratio

H = Exposed fin half-span

r = Density of air, lbs/in³

C_R = Fin root chord, inches

I = Fin taper ratio

C_{av} = Average chord, inches

$$= C_R \frac{(1+I)}{2}$$

A = Aspect ratio

$$= \frac{4H}{(1+I)C_R}$$

K_B = Bending frequency parameter, see Table 2

M_B = Apparent mass ratio for bending mode

$$= \frac{\rho}{8} \left(\frac{r}{r_m} \right) \left[\frac{(1+I)}{t} C_R \right]$$

Natural Frequency in Torsion –

The natural frequency in torsion can be estimated using the following equation.

$$w_q = K_T \left[\frac{CGg}{r_m I_P (1+M_T)} \right]^{1/2} \left[\frac{\rho}{2H} \right], \text{ Radians per Second}$$

Where,

C = Torsion constant of cross-section, in⁴

$$= \frac{C_{av}^3 t^3}{(t^2 + C_{av}^2)} \left[0.28 + 0.0534e^{-1/0.243C_{av}} \right]$$

I_P = Polar area moment-of-inertia, in⁴

$$= \frac{tC_{av}(C_{av}^2 + t^2)}{12}$$

K_T = Torsion frequency parameter, see Table 2

M_T = Apparent mass ratio for torsion mode

$$= \frac{3p}{64} \left(\frac{r}{r_m} \right) \left[\frac{(1+I)}{t} C_R \right]$$

Guideline for Equation Implementation –

Values for the frequency parameter functions K_B and K_T can be found in Table 2 for the various fin materials. For each material K_B and K_T vary with fin aspect ratio and taper ratio. The values for K_B and K_T of Table 2 can be used to interpolate values of K_B and K_T for other combinations of aspect ratio and taper ratio, as long as the combination falls within the range bounded by the table.

Although the apparent mass of the surrounding air is accounted for in the natural frequency calculation, its effect will be minimal. If the surrounding fluid were denser than that of air, then the effect of the apparent mass of the fluid may be more significant. However, it would be acceptable to ignore the apparent mass of air without changing the answer appreciably. By ignoring the apparent mass, it is assumed that the natural frequencies of the fin flying in air are equivalent to the natural frequencies of a fin flying in a vacuum.

Table 2 – Bending and Torsion Parameters for Natural Frequency Estimations								
Material: Polystyrene								
Taper Ratio	Aspect Ratio = 1		Aspect Ratio = 2		Aspect Ratio = 3		Aspect Ratio = 4	
	K_B	K_T	K_B	K_T	K_B	K_T	K_B	K_T
0.000	5.514	6.229	6.414	3.123	6.907	2.700	7.165	2.440
0.200	4.611	3.098	5.255	2.508	5.482	2.220	5.593	2.053
0.400	4.109	2.471	4.346	2.013	4.399	1.806	4.412	1.692
0.600	3.921	2.153	4.049	1.724	4.091	1.554	4.095	1.463
0.800	3.649	1.873	3.705	1.493	3.701	1.355	3.705	1.284
1.000	3.417	1.653	3.432	1.324	3.427	1.211	3.422	1.154
Material: Balsa								
Taper Ratio	Aspect Ratio = 1		Aspect Ratio = 2		Aspect Ratio = 3		Aspect Ratio = 4	
	K_B	K_T	K_B	K_T	K_B	K_T	K_B	K_T
0.000	4.180	5.563	5.171	4.378	5.736	3.834	6.112	3.500
0.200	3.591	4.505	4.305	3.635	4.686	3.224	4.908	2.953
0.400	3.432	3.933	3.971	3.051	4.213	2.673	4.336	2.437
0.600	3.358	3.640	3.763	2.643	3.902	2.260	3.961	2.049
0.800	3.299	3.422	3.583	2.318	3.652	1.948	3.678	1.767
1.000	3.192	3.125	3.393	2.035	3.434	1.708	3.449	1.557
Material: Basswood								
Taper Ratio	Aspect Ratio = 1		Aspect Ratio = 2		Aspect Ratio = 3		Aspect Ratio = 4	
	K_B	K_T	K_B	K_T	K_B	K_T	K_B	K_T
0.000	4.109	5.459	5.032	4.272	5.563	3.732	5.912	3.398
0.200	3.517	4.413	4.179	3.544	4.530	3.128	4.731	2.852
0.400	3.354	3.831	3.843	2.960	4.062	2.579	4.169	2.342
0.600	3.277	3.527	3.633	2.547	3.753	2.168	3.803	1.962
0.800	3.216	3.297	3.453	2.220	3.509	1.864	3.529	1.689
1.000	3.109	2.996	3.268	1.943	3.300	1.633	3.311	1.489

Example Problem –

The following is an example calculation of flutter speed for a fin made of polystyrene, typical of the plastic material used in commercially available model rockets. The required data for the natural frequency estimations are given below:

$$\mathbf{I} = \frac{2}{3} = \text{Chord taper ratio}$$

$$\mathbf{H} = 3.75 = \text{Exposed fin half span, inches}$$

$$t = 0.0083 = \text{Fin thickness, ft or 0.10-inches}$$

$$C_R = 3 = \text{Fin root chord, inches}$$

$$\mathbf{r}_m = 65.664 = \text{Density of fin material, lbs./cu-ft}$$

$$\mathbf{r} = 0.07647 = \text{Density of air, lbs./cu-ft}$$

$$a_o = 1116.4 = \text{Speed of sound in air, ft/s}$$

Step #1 – Calculate average chord of plan form.

$$C_{av} = (1 + \mathbf{I}) \frac{C_R}{2} = \left(1 + \frac{2}{3}\right) \left(\frac{3}{2}\right) = 2.5$$

Step #2 – Calculate the aspect ratio of the “mirrored” exposed fin plan form.

$$A = \frac{4H}{(1 + \mathbf{I})C_R} = \frac{(4)(3.75)}{\left(1 + \frac{2}{3}\right)(3)} = 3$$

Step #3 – From the above calculated aspect ratio (A) and the given taper ratio (\mathbf{I}), the frequency parameters can be interpolated from the data of Table 2 for the Polystyrene material. Data exists in Table 2 for the case of $A = 3$ and $\mathbf{I} = 2/3$, therefore there is no need for interpolation. Thus,

$$K_B = 3.961$$

$$K_T = 1.488$$

Step #4 – Calculate the apparent mass of the air for the bending mode.

$$M_B = \frac{\mathbf{p}}{8} \left(\frac{\mathbf{r}}{\mathbf{r}_m} \right) \left[\frac{(1 + \mathbf{I})}{t} C_R \right]$$

$$= \frac{\mathbf{p}}{8} \left(\frac{0.07647}{65.664} \right) \left[\frac{\left(1 + \frac{2}{3}\right)}{0.10} (3) \right] = 0.02287$$

Step #5 – Enough information is available to estimate the natural frequency in bending (plunging).

$$\begin{aligned} w_h &= K_B \left[\frac{Et^2 g}{12 r_m (1-n^2)(1+M_B)} \right]^{1/2} \left[\frac{1}{H^2} \right], \text{ Radians per Second} \\ &= 3.961 \left[\frac{(365000)(0.10)^2(386.088)}{12(0.038)[1-(0.33)^2](1+0.02287)} \right]^{1/2} \left[\frac{1}{(3.75)^2} \right] = 519 \text{ Radians / Second} \end{aligned}$$

Step #6 – Calculate the apparent mass of the air for the torsion mode.

$$\begin{aligned} M_T &= \frac{3p}{64} \left(\frac{r}{r_m} \right) \left[\frac{(1+I)}{t} C_R \right] \\ &= \frac{3p}{64} \left(\frac{0.07647}{65.664} \right) \left[\frac{(1+2/3)}{0.10} (3) \right] = 0.008575 \end{aligned}$$

Step #7 – Calculate the Polar area moment-of-inertia.

$$\begin{aligned} I_P &= \frac{t C_{av} (C_{av}^2 + t^2)}{12}, \text{ in}^4 \\ &= \frac{(0.10)(2.5)[(2.5)^2 + (0.10)^2]}{12} = 0.13041 \end{aligned}$$

Step #8 – Calculate the torsion constant of cross-section.

$$\begin{aligned} C &= \frac{C_{av}^3 t^3}{(t^2 + C_{av}^2)} \left[0.28 + 0.0534 e^{-0.243 C_{av}} \right] \\ &= \frac{(2.5)^3 (0.10)^3}{[(0.10)^2 + (2.5)^2]} \left[0.28 + 0.0534 e^{-0.10/0.243(2.5)} \right] = 0.0008118 \end{aligned}$$

Step #9 – Finally, enough information exists to estimate the natural frequency in torsion.

$$\begin{aligned} w_q &= K_T \left[\frac{CGg}{r_m I_P (1+M_T)} \right]^{1/2} \left[\frac{p}{2H} \right], \text{ Radians per Second} \\ &= 1.488 \left[\frac{(0.000979)(137220)(386.088)}{(0.038)(0.22525)(1+0.00857)} \right]^{1/2} \left[\frac{p}{2(3.75)} \right] = 1828 \text{ Radians / Second} \end{aligned}$$

The calculated natural (fundamental) frequencies compare well with that of the Finite Element results given in Figure 1 below.

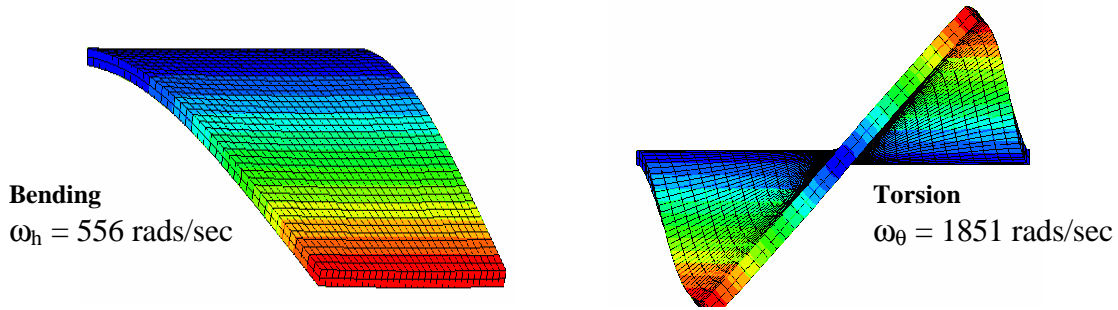


Figure 1 – The first (bending) and second (torsion) fundamental mode shapes as determined from FEA, corrected for the fluid apparent mass.

The natural frequency in bending of 519 radians per second and in torsion of 1828 radians per second are used in the sections on quasi-steady and unsteady flutter analysis to estimate the fin's flutter speed.

Reduced Frequency k -

Throughout this chapter the term "reduced frequency" will be used to define the applicability of simplifying assumptions to flutter calculations. The reduced frequency is the ratio of the frequency of vibration to a reference frequency defined by the linear flight speed divided by 1/2 the fin chord length. A very small value of reduced frequency ($k \ll 1.0$) represents a slow flapping and twisting motion of the fin relative to the linear flight speed of the fin. This occurs during supersonic and hypersonic speeds, and seldom within subsonic and transonic speeds. A larger value of reduced frequency ($k > 0.10$) represents a rapid rate of vibration relative to the linear flight speed of the fin, and is typical of what one would expect for the subsonic and transonic speeds. In equation form, the reduced frequency is given as:

$$k = \frac{(\mathbf{w})(c)}{2U_o},$$

Where:

\mathbf{w} = Frequency of Vibration

c = Fin Chord Length

U_o = Fin Linear Flight Speed

Two categories of flutter will be discussed in this chapter, that of quasi-steady flutter ($0 < k < 0.10$) and then a more general flutter analysis ($k > 0.0$).

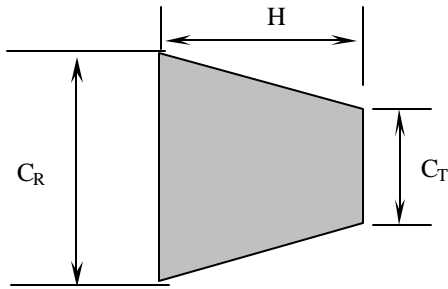
Quasi-Steady Flutter ($0 < k < 0.10$) -

In quasi-steady flutter, the frequency of vibration associated with the flapping and twisting of the fin is small relative to its linear flight speed. This can occur during supersonic and hypersonic speeds and seldom during subsonic and transonic speeds. Nevertheless, due to its simplicity in formulation this is an ideal place to start in the effort to understand the physics of flutter.

Geometry and aerodynamic considerations will be revisited prior to the derivation of the flutter equations.

Geometry -

The geometry of the fin and analysis space will be defined before pursuing a discussion of the quasi-steady aerodynamics and flutter equations. For aerodynamic considerations the plan-form geometry is as shown below:



Where,

H = exposed fin half span

C_R = exposed fin root chord

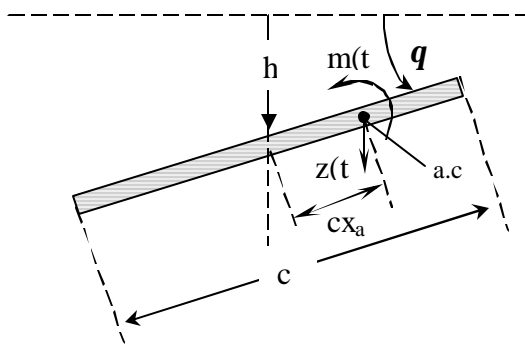
C_T = exposed fin tip chord

Then:

$$I = \frac{C_T}{C_R} = \text{Taper Ratio}$$

$$A = \frac{4H}{(1+I)C_R} = \text{Aspect Ratio}$$

The geometry for quasi-steady flutter as denoted in the cross-section perspective includes a plunging degree-of-freedom (h) and a rotational degree-of-freedom (q). The center-of-gravity and shear centers are assumed to reside along a spanwise line located at midchord ($c/2$). The aerodynamic center is assumed to be forward of the midchord by a distance of cX_a . The quasi-steady aerodynamic normal force $z(t)$ and moment $m(t)$ act at the aerodynamic center (a.c.). This geometry is illustrated below.



h = plunging degree-of-freedom

q = rotational degree-of-freedom

c = section chord length

X_a = distance of the aerodynamic center ahead of the midchord as a fraction of the chord length.

$z(t)$ = aerodynamic normal force

$m(t)$ = aerodynamic moment

Quasi-Steady Aerodynamics –

The quasi-steady aerodynamic approximation assumes:

1. That the phase angle between the normal force and angle-of-attack is negligible.
2. That any normal force due to the plunging motion is negligible.
3. That the unsteady pitching moment about the aerodynamic center is negligible.
4. That although the fin aspect ratio may be small, the amplitude of fin vibration in pitch (twist) is sufficiently small to allow for a linear approximation of the lift-curve slope.

The angle-of-attack (\mathbf{a}) is equivalent to the rotational angle (\mathbf{q}) within the restrained system just described. Also, the unsteady pitching moment about the aerodynamic center is zero since the quasi-steady force acts at the aerodynamic center. The quasi-steady normal force and moment are given as:

$$z(t) = -C_{La} \mathbf{a}(t) \mathbf{r} U_o^2 \frac{c}{2} = -C_{La} \mathbf{q}(t) \mathbf{r} U_o^2 \frac{c}{2}$$

$$m(t) = 0$$

Where,

C_{La} = 3D Lift-Curve Slope

\mathbf{r} = Density of Air

The 3D lift-curve slope is an adjustment to the theoretical 2D value of $2\mathbf{p}$, corrected for fin aspect ratio and compressibility. The Prandtl-Glauert correction for compressibility is applied to the Helmbold equation that corrects the 2D lift-curve slope for aspect ratio effects (Reference 2). The resulting equation is applicable to fins having thickness-to-chord ratios of 9% or less, and is reasonably accurate for speeds up to high subsonic Mach numbers ($M = 0.8$).

$$C_{La} = \frac{2\mathbf{p}A}{2 + \sqrt{A^2 + 4 - \left(A \frac{U_o}{a_o}\right)^2}} = \text{3D Lift-Curve Slope}$$

Where,

A = Fin Aspect Ratio

U_o = Fin Flight Speed

a_o = Speed of Sound

Solving for the Flutter Speed and Frequency –

The equations of motion associated with our system are given as follows:

$$m\ddot{h} + k_h h = -C_{La} \mathbf{q}(t) \mathbf{r} U_o^2 \frac{c}{2}$$

$$i_q \ddot{\mathbf{q}} + k_q \mathbf{q} = C_{La} \mathbf{q}(t) \mathbf{r} U_o^2 x_a \frac{c^2}{2}$$

Where,

m = Spanwise fin mass

k_h = Spanwise bending stiffness

i_q = Mass moment of inertia about fin mid-chord line

k_q = Spanwise torsional stiffness

Before solving the above system of differential equations, the following substitutions are made:

$$\mathbf{w}_h^2 = \frac{k_h}{m}, \text{ Where } \mathbf{w}_h = \text{Fin natural frequency in bending or plunging}$$

$$\mathbf{w}_q^2 = \frac{k_q}{i_q}, \text{ Where } \mathbf{w}_q = \text{Fin natural frequency in torsion or twist}$$

$$i_q = \frac{m c^2 r_q^2}{4}, \text{ Where } r_q = \text{Radius of gyration about the mid-chord line}$$

$$\mathbf{m} = \frac{4m}{\rho r c^2} = \text{Dimensionless airfoil-to-airstream mass ratio}$$

After making the above substitutions, the equations of motion are rewritten as:

$$\ddot{h} + \mathbf{w}_h^2 h = \frac{-2C_{La} \mathbf{q}(t) U_o^2}{\rho p c}$$

$$\ddot{\mathbf{q}} + \left[\mathbf{w}_q^2 - \frac{8C_{La} U_o^2 x_a}{r_q^2 \mathbf{m}^2 \rho} \right] \mathbf{q} = 0$$

The motion is assumed to be harmonic with the following form:

$$h = \bar{h} \cos \mathbf{w} t, \quad \text{Where } \bar{h} = \text{nominal plunging degree of freedom (eigenvector)}$$

$$\mathbf{q} = \bar{\mathbf{q}} \cos \mathbf{w} t, \quad \text{Where } \bar{\mathbf{q}} = \text{nominal torsional degree of freedom (eigenvector)}$$

Where \mathbf{w} = Frequency of vibration of coupled motion (eigenvalue)

After substituting the above solutions along with their 2nd derivatives into the equations of motion, the new system of linear equations can be expressed in matrix form as follows:

$$\begin{bmatrix} (\mathbf{w}_h^2 - \mathbf{w}^2) & \frac{2C_{La} U_o^2}{\rho p c} \\ 0 & \left(\mathbf{w}_q^2 - \mathbf{w}^2 - \frac{8C_{La} U_o^2 x_a}{r_q^2 \mathbf{m}^2 \rho} \right) \end{bmatrix} \begin{pmatrix} \bar{h} \\ \bar{\mathbf{q}} \end{pmatrix} = \begin{pmatrix} 0 \\ 0 \end{pmatrix}$$

Given that the eigenvectors are nonzero, then to satisfy the above system of equations the determinant of the 2x2 matrix must equal zero. The result is a 4th order characteristic equation in \mathbf{w} .

$$\mathbf{w}^4 + \mathbf{w}^2 \left(\frac{8C_{La} U_o^2 x_a}{r_q^2 \mathbf{m}^2 \rho} - \mathbf{w}_q^2 - \mathbf{w}_h^2 \right) + \left(\mathbf{w}_h^2 \mathbf{w}_q^2 - \frac{\mathbf{w}_h^2 8C_{La} U_o^2 x_a}{r_q^2 \mathbf{m}^2 \rho} \right) = 0$$

There are four solutions to the above 4th order characteristic equation, but only two unique positive solutions of \mathbf{W} . The two solutions are denoted as \mathbf{W}_1 and \mathbf{W}_2 , and are given as follows:

$$\mathbf{w}_1 = \mathbf{w}_h$$

$$\mathbf{w}_2 = \frac{\left[\mathbf{m}\mathbf{p}(\mathbf{w}_q^2 r_q^2 \mathbf{m}^2 \mathbf{p} - 8C_{La} U_o^2 x_a) \right]^{1/2}}{c r_q \mathbf{m}\mathbf{p}}$$

One solution to the vibration frequency equation, specific to this problem, is the natural bending frequency. This is a consequence of a straight tapered fin of constant thickness and homogenous isotropic material. That is, the configuration is absent of a mass imbalance and the shear center lies on the mid-chord coincident with the spanwise center-of-gravity distribution. Also, damping has been excluded from the analysis.

By definition, the flutter velocity is associated with the coalescence of the two frequencies into a single frequency, that is when $\mathbf{W}_1 = \mathbf{W}_2$. The coalescence of the two frequencies marks the boundary between damped and undamped vibration, characterized by a neutrally stable oscillation. For this particular problem, the flutter frequency is simply the natural bending frequency. The flutter velocity is easily obtained by equating the two frequencies and solving for the velocity, giving:

$$V_F = U_o(\mathbf{w}_1 = \mathbf{w}_2) = \sqrt{\frac{\mathbf{p}c^2 r_q^2 \mathbf{m}(\mathbf{w}_q^2 - \mathbf{w}_h^2)}{8C_{La} x_a}} = \text{Flutter Speed}$$

$$\mathbf{w}_F = \mathbf{w}_h = \text{Flutter Frequency}$$

In the case of $\mathbf{w}_h \ll \mathbf{w}_q$, the equation for flutter velocity can be simplified to:

$$V_F = U_o(\mathbf{w}_1 = \mathbf{w}_2) = \sqrt{\frac{\mathbf{p}c^2 r_q^2 \mathbf{m}\mathbf{w}_q^2}{8C_{La} x_a}}$$

In most cases $\mathbf{w}_h \ll \mathbf{w}_q$ will not be satisfied and the use of the above equation can lead to over prediction of the flutter speed. The error as a percent increase in flutter speed is calculated as follows:

$$\% \text{ - error} = \left[\frac{\mathbf{w}_q}{\sqrt{\mathbf{w}_q^2 - \mathbf{w}_h^2}} - 1 \right] \times 100$$

The dimensionless parameters of airfoil-to-airstream mass ratio and radius of gyration facilitated the ease in derivation of the flutter speed equation, however they can be foreign concepts to many of us. To restate the flutter speed equation in terms of more familiar physical quantities the following substitutions are made:

$$r_q^2 = \frac{4i_q}{mc^2}, \quad m = \frac{4m}{\rho rc^2}, \quad i_q = \frac{\mathbf{r}_m ct}{12}(t^2 + c^2)$$

After making these substitutions and simplifying, the quasi-steady flutter equation becomes:

$$\longrightarrow V_F = U_o(\mathbf{w}_1 = \mathbf{w}_2) = \sqrt{\frac{\mathbf{r}_m t(t^2 + c^2)(\mathbf{w}_q^2 - \mathbf{w}_h^2)}{6\rho r C_{La} x_a}} = \text{Quasi-Steady Flutter Speed!}$$

Where,

\mathbf{r}_m = Mass density of fin material

\mathbf{r} = Mass density of air

c = Fin average chord

t = Fin thickness

\mathbf{w}_q = Fin natural frequency in torsion or twist

\mathbf{w}_h = Fin natural frequency in bending or plunging

C_{La} = 3D Lift-curve slope

x_a = Fractional distance of aerodynamic center ahead of mid-chord

The reduced frequency at flutter, and *specific to the fin configurations of this study*, can be defined in terms of the natural bending frequency and the flutter velocity. The result can be compared to the criteria for quasi-steady flutter to determine the validity of using this approach for predicting flutter speed.

$$k_F = \frac{\mathbf{w}_F c}{2V_F} = \frac{\mathbf{w}_h c}{2V_F} = \text{Reduced Frequency at Flutter}$$

Recall that the fin free-stream velocity is included in the calculation of the 3D lift-curve slope. For flutter calculations this velocity is the same as the flutter speed. However, the 3D lift-curve slope is used in the calculation of the flutter speed. So, how does one calculate flutter speed when its value is needed for its calculation? To solve this dilemma, a function is defined given by the ratio of the 3D compressible flutter speed to that of the 2D incompressible flutter speed. Let the 2D incompressible flutter speed be designated as V_{2D} and the 3D compressible flutter speed designated as V_{3D} . The ratio is then given as:

$$\frac{V_{3D}}{V_{2D}} = \left[\frac{2 + \sqrt{A^2 + 4 - \left(A \frac{V_{3D}}{a_o}\right)^2}}{A} \right]^{\frac{1}{2}}$$

The above equation can be rearranged to yield the following quartic equation in V_{3D} .

$$A^2 V_{3D}^4 - V_{2D}^2 \left[2 + \sqrt{A^2 + 4 - \left(A \frac{V_{3D}}{a_o} \right)^2} \right]^2 = 0$$

The above equation has four solutions for V_{3D} . They are given as follows:

$$V_{3D} = \begin{bmatrix} V_{3D}(1) \\ V_{3D}(2) \\ V_{3D}(3) \\ V_{3D}(4) \end{bmatrix} = \frac{V_{2D}}{2Aa_o} \begin{bmatrix} \left\{ -2A \left[AV_{2D}^2 - 4a_o^2 - \left(A^2 V_{2D}^4 - 8AV_{2D}^2 a_o^2 + 16a_o^4 + 4A^2 a_o^4 \right)^{1/2} \right] \right\}^{1/2} \\ - \left\{ -2A \left[AV_{2D}^2 - 4a_o^2 - \left(A^2 V_{2D}^4 - 8AV_{2D}^2 a_o^2 + 16a_o^4 + 4A^2 a_o^4 \right)^{1/2} \right] \right\}^{1/2} \\ \left\{ -2A \left[AV_{2D}^2 - 4a_o^2 + \left(A^2 V_{2D}^4 - 8AV_{2D}^2 a_o^2 + 16a_o^4 + 4A^2 a_o^4 \right)^{1/2} \right] \right\}^{1/2} \\ - \left\{ -2A \left[AV_{2D}^2 - 4a_o^2 + \left(A^2 V_{2D}^4 - 8AV_{2D}^2 a_o^2 + 16a_o^4 + 4A^2 a_o^4 \right)^{1/2} \right] \right\}^{1/2} \end{bmatrix}$$

The first solution $V_{3D}(1)$ is a positive real root. The second solution $V_{3D}(2)$ is a negative real root and equal in magnitude to $V_{3D}(1)$. The third solution $V_{3D}(3)$ is a positive imaginary root. The fourth solution $V_{3D}(4)$ is a negative imaginary root and equal in magnitude to $V_{3D}(3)$. Thus, $V_{3D}(1)$ is the only solution that has any physical meaning. Therefore, the 3D compressible flutter speed can be expressed in terms of the 2D incompressible flutter speed, aspect ratio and the speed of sound. The 3D lift-coefficient and subsonic compressibility are accounted for in closed form. In summary, the 3D incompressible flutter speed for the quasi-steady case is given as:

$$V_{3D} = \frac{V_{2D}}{2Aa_o} \left\{ -2A \left[AV_{2D}^2 - 4a_o^2 - \left(A^2 V_{2D}^4 - 8AV_{2D}^2 a_o^2 + 16a_o^4 + 4A^2 a_o^4 \right)^{1/2} \right] \right\}^{1/2}$$

Where,

A = Fin Projected Aspect Ratio

a_o = Speed of Sound

$$V_{2D} = \sqrt{\frac{\mathbf{r}_m t (t^2 + c^2) (\mathbf{w}_q^2 - \mathbf{w}_h^2)}{12c\mathbf{r}p\mathbf{x}_a}} = 2D \text{ incompressible flutter speed}$$

A convenient form of the above equation is to cast it in terms of Mach number ratio R_M . This relation is given as follows:

$$R_M = \frac{M_{3D}}{M_{2D}} = \frac{1}{2A} \left\{ -2A \left[AM_{2D}^2 - 4 - \left(A^2 M_{2D}^4 - 8AM_{2D}^2 + 16 + 4A^2 \right)^{1/2} \right] \right\}^{1/2}$$

Where,

$$M_{2D} = \frac{V_{2D}}{a_o} = 2D \text{ incompressible Mach number at flutter speed}$$

$$M_{3D} = \frac{V_{3D}}{a_o} \quad \text{3D compressible Mach number at flutter speed}$$

The above relation can be plotted as a function of aspect ratio for several 2D incompressible Mach numbers, resulting in a family of curves that could be quite useful. These curves are illustrated in Figure 2.

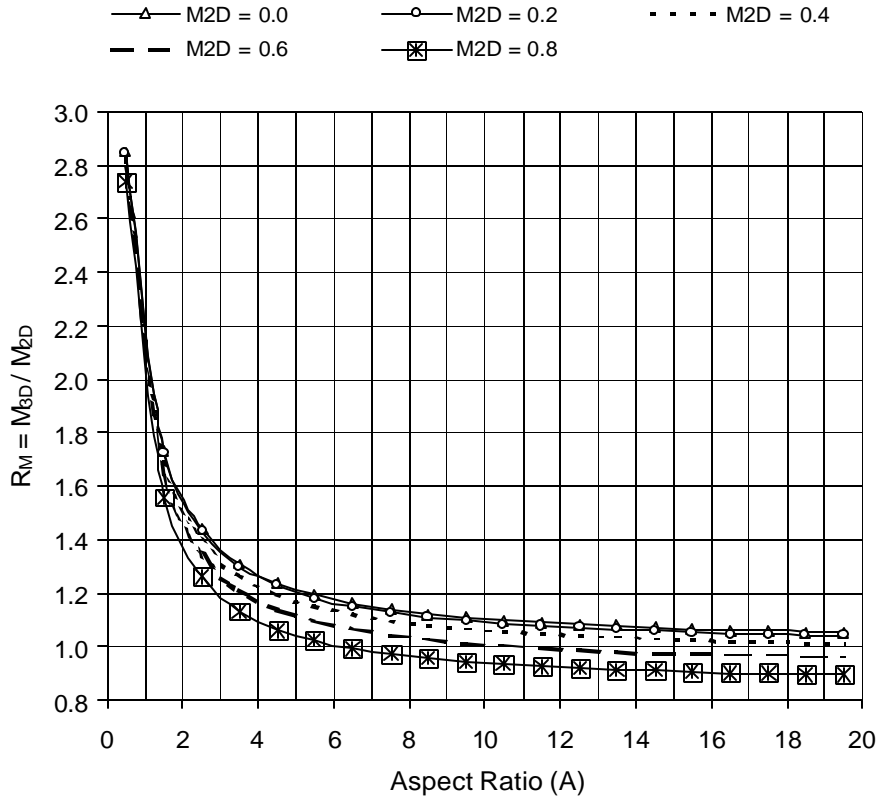


Figure 2 – Mach number ratio (R_M) versus aspect ratio for various M_{2D}

Discussion on the prediction of flutter speed will be limited to subsonic flight ($M \leq 0.8$) for the following reasons:

1. The accuracy of the conversion from V_{2D} (or M_{2D}) to V_{3D} (or M_{3D}) diminishes as transonic Mach Numbers are approached ($0.8 \leq M \leq 1.2$). In fact, the conversion presented here becomes imaginary at a Mach Number of unity or above.
2. Recall that the quasi-steady method becomes more accurate as the fundamental frequency becomes small ($k \leq 0.1$), which occurs more frequently for transonic and supersonic flight. One might conclude that this simplifies the flutter calculation. However, aerodynamics becomes considerably more complicated due to the presence of compression or shock waves. Both airfoil and planform geometry influence the development of compression or shock waves. Portions or all of the fin may or may not be immersed in supersonic flow, depending on fin geometry, flow interaction with adjacent parts, free-stream Mach Number and fin incidence with the free stream flow. There is no convenient and simple approach to predict the slope of the lift-coefficient versus angle-of-attack (C_{La}) in transonic and supersonic speeds.

The polystyrene fin described in the natural frequency calculation is revisited for the calculation of flutter speed. This example utilizes the natural frequencies previously estimated. The pertinent data is given below:

$$\begin{aligned}
 A &= 3 = \text{Fin planform aspect ratio} \\
 t &= 0.0083 = \text{Fin thickness, ft} \\
 c &= 0.208 = \text{Average chord, ft} \\
 x_a &= 0.25 = \text{Fractional distance of aerodynamic center ahead of mid-chord} \\
 \mathbf{r} &= 0.07647 = \text{Density of air, lbs./cu-ft} \\
 a_o &= 1116.4 = \text{Speed of sound in air, ft/s} \\
 \mathbf{w}_h &= 519 = \text{Bending or plunging natural frequency corrected for the apparent mass} \\
 &\quad \text{of the fluid, Radians per Second} \\
 \mathbf{w}_q &= 1828 = \text{Torsion or twisting natural frequency corrected for the apparent} \\
 &\quad \text{mass of the fluid, Radians per Second} \\
 \mathbf{r}_m &= 65.664 = \text{Density of fin material, lbs/cu-ft}
 \end{aligned}$$

Step #1 – Calculation of the 2D incompressible flutter speed

$$\begin{aligned}
 V_{2D} &= \sqrt{\frac{\mathbf{r}_m t (t^2 + c^2) (\mathbf{w}_q^2 - \mathbf{w}_h^2)}{12 c \mathbf{r} p x_a}} \\
 &= \sqrt{\frac{(65.664)(0.0083) [(0.0083)^2 + (0.208)^2] [(1828)^2 - (519)^2]}{12(0.208)(0.07647)(p)(0.25)}} = 698 \text{ ft/s} = 476 \text{ mph}
 \end{aligned}$$

Step #2 – Substitute $V_{2D} = 476 \text{ mph}$ into the equation for V_{3D} , yielding,

$$\begin{aligned}
 V_{3D} &= \frac{V_{2D}}{2A a_o} \left\{ -2A \left[A V_{2D}^2 - 4a_o^2 - (A^2 V_{2D}^4 - 8A V_{2D}^2 a_o^2 + 16a_o^4 + 4A^2 a_o^4)^{1/2} \right] \right\}^{1/2} \\
 &= 876 \text{ ft/s} = 597 \text{ mph}
 \end{aligned}$$

The reduced frequency at flutter speed can be calculated and compared to the criteria for quasi-steady flutter.

$$K_F = \frac{\mathbf{w}_h c}{2V_F} = \frac{(519)(0.208)}{(2)(876)} = 0.062 = \text{Reduced frequency at flutter}$$

Recall that the criterion for quasi-steady flutter is $K < 0.10$. The value of $K = 0.062$ falls within the criteria for quasi-steady flutter, thus suggesting that the prediction may be within reason.

Finally, the degree of error can be determined if it were assumed that the bending or plunging natural frequency is negligible in the flutter velocity equation. Recall that this error is determined by:

$$\% \text{ - error} = \left[\frac{W_q}{\sqrt{W_q^2 - W_h^2}} - 1 \right] \times 100.$$

Then for this problem the error is:

$$\% \text{ - error} = \left[\frac{1828}{\sqrt{(1828)^2 - (519)^2}} - 1 \right] \times 100 = 4.3\%$$

That is, if we ignore the bending natural frequency, then the flutter speed would be over-predicted by 4.3% relative to a calculation that accounts for this frequency. The error tends to increase as fin aspect ratio decreases and fin taper ratio increases. Errors on the order of 20% to 40% are possible.

Unsteady Flutter Analysis –

The unsteady flutter analysis presented here is applicable to all values of reduced frequency ($0 \leq k \leq \infty$). This approach includes the effects of "artificial" structural damping and unsteady aerodynamics. Detailed theory and equation development is beyond the scope of this discussion. Presentation of the method begins with the characteristic equation of the complex frequency with the effects of damping and unsteady aerodynamics included. But first, physical interpretations of the "artificial" structural damping and unsteady aerodynamics will be discussed.

Artificial Structural Damping -

Structural damping was included in the formulation of the torsion and bending equations of motion. To facilitate the ease in development of the characteristic equation of the complex frequency, it is assumed that the damping in both torsion and bending are equal. In reality this is not the case. However, recall that flutter is associated with a value of zero damping which is the boundary between damped motion and divergent motion. Although flutter may be the coupled motion between torsion and bending modes, flutter occurs at the lower velocity associated with the mode that exhibits zero damping first. Typically, the mode to first exhibit zero damping is torsion. For purposes of determining the flutter speed, non-zero values of the damping are not important. Damping is calculated as a consequence of the analysis, but because it has no quantitative significance it is referred to as "artificial" structural damping. As will be demonstrated later, the flutter analysis consists of searching for the reduced frequency (k) that produces zero damping for each mode. This iterative approach produces plots of "artificial" structural damping versus flight velocity for each mode. In short, the "artificial" structural damping is included in the analysis solely to facilitate the calculation of a solution to the flutter problem.

Unsteady Aerodynamics -

In steady 2-dimensional aerodynamics, lift around an airfoil is developed from circular airflow that is "bound" to that airfoil. This circular flow arises from the fact that the air over the upper surface of the airfoil moves faster than air moving past the airfoil's lower surface. In order for a net force to be developed, the airflow on the upper surface must meet the airflow on the lower surface at the airfoil's trailing edge as a tangential streamline to the airfoils mean camber line. That is, the local circulation and

pressure jump at the trailing edge are zero. This condition of zero pressure-jump across the trailing edge is known as the Kutta condition. For the case of a net force, integration of the velocity component tangent to the airfoil's surface about a closed loop comprising the airfoil's shape will result in a nonzero value, known as the total circulation " Γ ". The Kutta-Joukowski Law states that an airfoil's lift is proportional to the total circulation per the following relation,

$$l = \rho V \Gamma, \text{ 2-dimensional lift}$$

Where,

ρ = Density of Air

V = Free Stream Velocity

Γ = Strength of Circulation

There exists a unique value of circulation for an airfoil traveling at a given velocity with a given angle-of-attack. This circulation is described as "bound" to the airfoil for the case of steady flow. When an airfoil is brought up to speed at an angle-of-attack, it sheds a vortex downstream into its wake. The strength of this vortex is equal in magnitude to that of the circulation developed and "bound" to the airfoil. When perturbed to a new state (i.e.; velocity and/or angle-of-attack), another vortex is shed into the airfoil's wake equal in strength to the difference in the previous "bound" circulation and the newly developed "bound" circulation.

The unsteady 2-dimensional aerodynamics associated with flutter is traditionally characterized by a continuous harmonic oscillation in pitch and plunging degrees-of-freedom about a steady state condition. In reference to the previous discussion about vortex shedding, it can be imagined that two vortices are shed during each cycle.

The vorticity that shed into the airfoil's wake is simply convected with the flow; thus it does not change with time or position. Mathematically we say its total derivative is zero. Metaphorically, wake vorticity has been described as being like the product of the expulsion of intestinal gas, it stays in one place and lasts a long time. Recall that the Kutta condition requires a zero pressure jump across the trailing edge of the airfoil, and for steady flow this is equivalent to zero local vorticity at the trailing edge. Although vorticity exists at the trailing edge and in the wake for unsteady flow, the Kutta condition is still satisfied because there does not exist a surface that can sustain a pressure difference. Essentially, the end result is that for unsteady flow the vorticity distribution is continuous over the domain of airfoil and wake. Thus, analytical and numerical solutions are possible for describing unsteady flow over airfoils and wings.

One of the earliest and most notable closed-form analytical solutions to unsteady flow about a 2-dimensional airfoil is that of Theodorsen (1935). Theodorsen characterizes the unsteady aerodynamics as complex quantities in normal force and moment, and are functions of the reduced frequency of motion. Likewise, the pitching and plunging motions at the quarter-chord of the airfoil are characterized as complex functions as well. The details of Theodorsen's solution are beyond the scope of this discussion, but are found in Reference 3. His results and their application to the problem described in the quasi-steady section are presented here. The Theodorsen aerodynamic functions are given as follows.

$$\begin{aligned} L_a &= \text{Oscillatory lift due to pitch motion} \\ &= \frac{1}{2} - i \left(\frac{1}{k} \right) \left[1 + 2(F + iG) \right] - 2 \left(\frac{1}{k} \right)^2 (F + iG) \end{aligned}$$

$$\begin{aligned} L_h &= \text{Oscillatory lift due to plunging motion} \\ &= 1 - 2i \left(\frac{1}{k} \right) (F + iG) \end{aligned}$$

$$M_a = \text{Oscillatory moment due to pitch motion}$$

$$= \frac{3}{8} - i\left(\frac{1}{k}\right)$$

$$M_h = \text{Oscillatory moment due to plunging motion}$$

$$= \frac{1}{2}$$

F and G are the in-phase and out-of-phase components of the Theodorsen Circulation Function for harmonic motion, respectively. Values for F and G as a function of reduced frequency k are given in Table 3.0 for 2-dimensional incompressible flow about an airfoil.

Table 3 - Components of Theodorsen Circulation Function for Harmonic Motion						
k	$F(k)$	$-G(k)$		k	$F(k)$	$-G(k)$
0.000	1.0000000	0.0000000		0.260	0.6865125	0.1842043
0.002	0.9967096	0.0125797		0.280	0.6752491	0.1818807
0.004	0.9932579	0.0222566		0.300	0.6649711	0.1793191
0.006	0.9897082	0.0307752		0.320	0.6555686	0.1765929
0.008	0.9860897	0.0385130		0.340	0.6469460	0.1737580
0.010	0.9824215	0.0456521		0.360	0.6390200	0.1708575
0.012	0.9787174	0.0523015		0.380	0.6317179	0.1679244
0.014	0.9749880	0.0585345		0.400	0.6249763	0.1649840
0.016	0.9712418	0.0644043		0.450	0.6102237	0.1577173
0.018	0.9674856	0.0699515		0.500	0.5797361	0.1507095
0.020	0.9637252	0.0752079		0.550	0.5875922	0.1440533
0.022	0.9599657	0.0801999		0.600	0.5788016	0.1377852
0.024	0.9562111	0.0849491		0.650	0.5712671	0.1319106
0.026	0.9524651	0.0894742		0.700	0.5647595	0.1264189
0.028	0.9487308	0.0937910		0.750	0.5590999	0.1212905
Table 3 - Components of Theodorsen Circulation Function for Harmonic Motion Cont'd						
k	$F(k)$	$-G(k)$		k	$F(k)$	$-G(k)$
0.030	0.9450110	0.0979135		0.800	0.5541466	0.1165024
0.040	0.9267018	0.1160013		0.850	0.5497866	0.1120301
0.050	0.9090090	0.1306444		0.900	0.5459286	0.1078496
0.060	0.8920397	0.1425944		0.950	0.5424983	0.1039377
0.070	0.8758427	0.1523817		1.000	0.5394348	0.1002729
0.080	0.8604318	0.1604021		1.100	0.5342147	0.0936062
0.090	0.8457992	0.1669615		1.200	0.5299560	0.0877089
0.100	0.8319241	0.1723022		1.300	0.5264367	0.0824643
0.110	0.8187779	0.1766195		1.400	0.5234957	0.0777759
0.120	0.8063273	0.1800727		1.500	0.5210132	0.0735641
0.130	0.7945372	0.1827933		2.000	0.5129548	0.0576913
0.140	0.7833715	0.1848904		2.500	0.5087440	0.0472969
0.150	0.7727946	0.1864556		3.000	0.5062800	0.0400039
0.160	0.7627719	0.1875659		4.000	0.5036709	0.0304961
0.170	0.7532699	0.1882865		5.000	0.5023972	0.0245986
0.180	0.7442570	0.1886727		10.000	0.5006178	0.0124467
0.190	0.7357031	0.1887718		20.000	0.5001558	0.0062432
0.200	0.7275799	0.1886242		50.000	0.5000250	0.0024996
0.220	0.7125211	0.1877232		100.000	0.5000062	0.0012499
0.240	0.6988879	0.1861940		∞	0.5000000	0.0000000

Solution to the Unsteady Flutter Problem –

The equations for unsteady flutter will be presented along with the solution to the 2-dimensional flutter problem solved in the quasi-steady analysis. To reiterate, the applicable data for this problem is given below:

$$\begin{aligned}
 t &= 0.0083 && \text{Fin thickness, in feet.} \\
 C_{av} &= 0.208 && \text{Fin average chord, in feet.} \\
 \mathbf{r} &= 0.07647 && \text{Density of air, lbs/cu-ft} \\
 \mathbf{r}_m &= 65.664 && \text{Density of fin material, lbs/cu-ft} \\
 \mathbf{w}_h &= 519 && \text{Fin natural frequency in plunging (bending), Radians per Second} \\
 \mathbf{w}_q &= 1828 && \text{Fin natural frequency in twist (torsion), Radians per Second}
 \end{aligned}$$

A correction to the natural frequency for the apparent mass of the air is not necessary for the unsteady problem. The apparent mass of the air is accounted for in the aerodynamic solution.

The first step involves the calculation of a dimensionless airfoil-to-airstream mass ratio and a dimensionless radius-of-gyration as follows:

$$\begin{aligned}
 \mathbf{m} &= \left(\frac{4}{\mathbf{p}} \right) \left(\frac{\mathbf{r}_m}{\mathbf{r}} \right) \left(\frac{t}{C_{av}} \right) = 43.731 \\
 r_q &= \sqrt{\frac{t^2 + C_{av}^2}{3C_{av}^2}} = 0.578
 \end{aligned}$$

The unsteady flutter solution involves several repetitive calculations, resulting in a graphical representation of artificial structural damping versus linear velocity for the torsion and bending modes. The flutter and divergence velocities are extracted from the curves representing the torsion and bending modes, respectively. To construct these curves, damping and velocity pairs for each mode $[(g_1, V_1), (g_2, V_2)]$ are calculated as a function of reduced frequency (k). Usually an initial value for reduced frequency is “guessed” or estimated from a quasi-steady analysis. As an example, let the initial value of reduced frequency be $k = 0.06$.

From Table 1.0, the values F and G for a reduced frequency of 0.06 are 0.8920397 and -0.1425944 , respectively. Given F and G , then the Theodorsen aerodynamic functions are calculated as:

$$\begin{aligned}
 L_a &= \frac{1}{2} - i \left(\frac{1}{k} \right) \left[1 + 2(F + Gi) \right] - 2 \left(\frac{1}{k} \right)^2 (F + Gi) = -499.831 + 32.818i \\
 L_h &= 1 - 2i \left(\frac{1}{k} \right) (F + Gi) = -3.753 - 29.735i \\
 M_a &= \frac{3}{8} - i \left(\frac{1}{k} \right) = 0.375 - 16.667i
 \end{aligned}$$

$$M_h = \frac{1}{2}$$

The coefficients to the characteristic equation of complex frequency ' Ω ' are functions of the dimensionless aerodynamic, mass and radius-of-gyration parameters. The characteristic equation is quadratic in Ω and thus has three coefficients. These coefficients are defined as follows:

$$A_1 = \left(\frac{m w_h r_q}{w_q} \right)^2 = 51.468$$

$$A_2 = m \left(\frac{w_h}{w_q} \right)^2 \left[\frac{1}{2} (L_a + M_h) - m_q^2 - M_a - \frac{L_h}{4} \right] - m_q^2 (L_h + m)$$

$$= -1.513 \times 10^3 + 576.934i$$

$$A_3 = L_h \left(M_a + \frac{m}{4} + m_q^2 \right) - L_a \left(\frac{m}{2} - M_h \right) + m \left(m_q^2 - \frac{M_h}{2} + M_a \right)$$

$$= 1.123 \times 10^4 - 217i$$

The two solutions to the complex frequency are a function of these coefficients. The solution having subscript '1' is typically associated with that of the bending (plunging) mode, and the solution having subscript '2' is typically associated with the torsion (twisting) mode. These solutions are given as follows :

$$\Omega_1 = \frac{-A_2 + \sqrt{A_2^2 - A_1 A_3}}{2A_1} = 21.543 - 14.566i, \text{ Complex Frequency in bending}$$

$$\Omega_2 = \frac{-A_2 - \sqrt{A_2^2 - A_1 A_3}}{2A_1} = 7.859 + 3.356i, \text{ Complex Frequency in torsion}$$

The frequency of vibration and artificial structural damping for each mode are calculated from their respective complex frequencies and the natural frequency in torsion, per the following equations:

$$w_1 = \frac{w_q}{\sqrt{\text{Re}(\Omega_1)}} = 393.842, \text{ frequency of vibration in bending, Hz.}$$

$$w_2 = \frac{w_q}{\sqrt{\text{Re}(\Omega_2)}} = 652.056, \text{ frequency of vibration in torsion, Hz.}$$

$$g_1 = \frac{\text{Im}(\Omega_1)}{\text{Re}(\Omega_1)} = -0.676, \text{ artificial structural damping in bending}$$

$$g_2 = \frac{\text{Im}(\Omega_2)}{\text{Re}(\Omega_2)} = 0.427, \text{ artificial structural damping in torsion}$$

Finally, the frequencies of vibration are converted to velocity by using half the average chord and the fundamental frequency.

$$V_1 = \frac{C_{av} w_1}{2.93k} = 466.196, \text{ linear velocity associated with bending mode, mph}$$

$$V_2 = \frac{C_{av} w_2}{2.93k} = 771.847, \text{ linear velocity associated with torsion mode, mph}$$

In summary of the first pass through the equations, for $k = 0.06$ the data pairs of velocity and damping for each mode are:

$$[k, (g_1, V_1), (g_2, V_2)] = [0.06, (-0.676, 466\text{mph}), (0.427, 772\text{mph})]$$

Several passes through the equations are made to find damping and velocity pairs for selected values of reduced frequency. After a sufficient number of pairs are generated, plots for each modal pair of artificial structural damping versus velocity are constructed. Sufficient number of points must exist to construct plots that intersect the horizontal axis, representing zero damping. The results for several passes through the equations for the example problem are given in Table 4 and plotted in Figure 3.

Table 4 – Example Problem Results After Several Passes Through the Equations				
	Bending Mode		Torsion Mode	
<i>k</i>	<i>g</i> ₁	<i>V</i> ₁ (mph)	<i>g</i> ₂	<i>V</i> ₂ (mph)
0.002	-0.029	486.	0.015	18360
0.006	-0.081	488.	0.045	6127
0.01	-0.130	490.	0.076	3685
0.02	-0.254	494	0.158	1866
0.03	-0.384	496	0.249	1280
0.05	-0.615	478	0.399	855
0.08	-0.670	405	0.388	631
0.13	-0.398	282	0.129	485
0.14	-0.351	263	0.087	472
0.15	-0.311	246	-0.052	461
0.16	-0.279	230	-0.024	452
0.17	-0.252	217	-0.001	443
0.18	-0.229	204	-0.017	435
0.20	-0.194	183	-0.042	418
0.22	-0.167	166	-0.057	402
0.26	-0.131	140	-0.071	371
0.36	-0.084	101	-0.067	303
0.50	-0.054	72	-0.051	235
0.80	-0.031	45	-0.027	154
1.10	-0.022	33	-0.018	113

2.00	-0.012	18	-0.009	63
3.00	-0.0076	12	-0.0058	42
5.00	-0.0045	7.2	-0.0034	25

Results of Example Problem

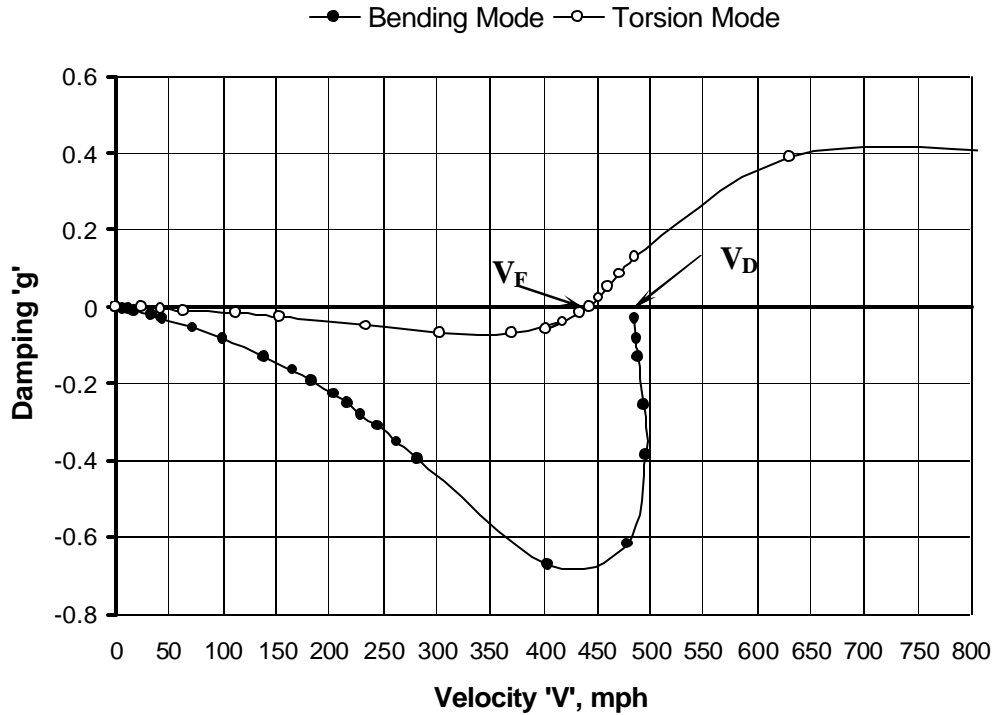


Figure 3 – Artificial Damping Versus Flight Velocity for each Mode

The curve for the torsion mode of Figure 3 crosses the abscissa first, defining the flutter speed (V_F) of 443-mph at zero artificial structural damping. Prior to 443-mph the fin motion is damped (negative g) in both torsion and bending modes. Above 443-mph the motion is divergent in torsion but remains damped in bending until approximately 485-mph. The curve for the bending mode crosses the abscissa at about 485-mph, defining the divergence speed (V_D). The divergence speed marks the boundary between fully or partially damped motion (at least one modal degree-of-freedom is damped) and completely divergent motion (all modal degrees-of-freedom are divergent, that is zero or positive g). If a fin has not structurally failed prior to the divergence speed, it will at or just above it.

It should be noted that this unsteady flutter analysis has been limited to 2-dimensional incompressible flow. If it were assumed that the relationship between the 3D compressible flutter speed and the 2D incompressible flutter speed for the quasi-steady case holds for the unsteady flutter case, then the 3D incompressible flutter speed for this example is,

$$\begin{aligned}
 V_{3D}(V_{2D} = 443\text{mph}) &= \frac{V_{2D}}{2Aa_o} \left\{ -2A \left[AV_{2D}^2 - 4a_o^2 - \left(A^2V_{2D}^4 - 8AV_{2D}^2a_o^2 + 16a_o^4 + 4A^2a_o^4 \right)^{1/2} \right] \right\}^{1/2} \\
 &= 825 \text{ ft/s} = 563 \text{ mph}
 \end{aligned}$$

It is doubtful the above relationship is valid for unsteady flutter. Unfortunately it is difficult to cast the unsteady flutter analysis into a 3-dimensional solution for low aspect ratio wings. With the advent of high-speed computers, most subsonic flutter analyses use more sophisticated aerodynamic tools such as Doublet Lattice Methods (DLM) and Computational Fluid Dynamics (CFD) coupled with structural analysis tools such as Finite Element Methods. These tools are well beyond the scope of this chapter, and their cost beyond the pocket books of most hobbyists. However, if one could produce tables of F and G for thin wings of various aspect ratios, taper ratios and operational Mach Numbers, then it may be possible to perform a flutter analysis in the same manner as that of the 2-dimensional example, without having to devise an unsubstantiated correction scheme for 3D incompressible effects as proposed above. It is conceivable that the data for these tables may be derived using an unsteady Doublet Lattice Method.

Final Assessment of Example Problem –

Recall that this example is limited to a straight fin of trapezoidal shape with zero static unbalance, and constructed from a homogeneous material. Also, the coupling of body dynamics and aero-elasticity with that of the fins was not considered. As such, the equations presented here have been simplified. Nevertheless the calculations and related discussion should have provided insight into the complexity of the flutter problem. The following summarizes the results of this problem.

Method	V_F (mph)	V_D (mph)	Reduced Frequency (k)
V_{2D} (Quasi-Steady)	476	Not calculated	0.078
V_{3D} (Quasi-Steady)	597	Not calculated	0.062
V_{2D} (Unsteady)	443	485	0.170
V_{3D} (Unsteady)	563	Not calculated	Not calculated

Some additional thoughts to consider before leaving the subject of flutter are:

1. The range between the prediction of flutter speed given by the 2-dimensional incompressible method and its correction for 3-dimensional compressible flow will decrease with an increase in fin aspect ratio and Mach number. Figure 2 illustrates this quite well.
2. The difference between flutter speed given by the quasi-steady method and the unsteady method tends to decrease with decreasing reduce frequency.
3. It is anticipated that coupling the body dynamics and aero-elastic behavior with that of the fins would tend to reduce flutter speed. It would be an interesting study to determine this effect by modeling an entire rocket structure and calculate the flutter speed, then compare the result to an isolated fin analysis as discussed in this study.

REFERENCES

1. Forest Products Laboratory, 1999. *Wood handbook—Wood as an engineering material*. Gen. Tech. Rep. FPL-GTR-113. Madison, WI: US Department of Agriculture, Forest Service, Forest Products Laboratory. Chapter 4.
2. McCormick B.W.: *Aerodynamics, Aeronautics, and Flight Mechanics*, Chapter 5 – *Lift and Drag at High Mach Numbers, Three-Dimensional Wings*, pp. 283-284, John Wiley & Sons Inc., 1979.
3. Luke, Yudell L., and Dengler, Max A. *Tables of the Theodorsen Function for Generalized Motion*. J. Aero. Science, 18, p. 478, 1951.